

# Next-to-Leading Order QCD Analysis of Polarized Deep Inelastic Scattering Data

E154 Collaboration

K. Abe<sup>t</sup>, T. Akagi<sup>q</sup>, B. D. Anderson<sup>g</sup>, P. L. Anthony<sup>q</sup>,  
 R. G. Arnold<sup>a</sup>, T. Averett<sup>e</sup>, H. R. Band<sup>v</sup>, C. M. Berisso<sup>h</sup>,  
 P. Bogorad<sup>n</sup>, H. Borel<sup>f</sup>, P. E. Bosted<sup>a</sup>, V. Breton<sup>b</sup>,  
 M. J. Buenerd<sup>q,1</sup>, G. D. Cates<sup>n</sup>, T. E. Chupp<sup>i</sup>, S. Churchwell<sup>h</sup>,  
 K. P. Coulter<sup>i</sup>, M. Daoudi<sup>q</sup>, P. Decowski<sup>o</sup>, R. Erickson<sup>q</sup>,  
 J. N. Fellbaum<sup>a</sup>, H. Fonvieille<sup>b</sup>, R. Gearhart<sup>q</sup>,  
 V. Ghazikhanian<sup>d</sup>, K. A. Griffioen<sup>u</sup>, R. S. Hicks<sup>h</sup>, R. Holmes<sup>r</sup>,  
 E. W. Hughes<sup>e</sup>, G. Igo<sup>d</sup>, S. Incerti<sup>b</sup>, J. R. Johnson<sup>v</sup>,  
 W. Kahl<sup>r</sup>, M. Khayat<sup>g</sup>, Yu. G. Kolomensky<sup>h</sup>, S. E. Kuhn<sup>l</sup>,  
 K. Kumar<sup>n</sup>, M. Kuriki<sup>t</sup>, R. Lombard-Nelsen<sup>f</sup>, D. M. Manley<sup>g</sup>,  
 J. Marroncle<sup>f</sup>, T. Maruyama<sup>q</sup>, T. Marvin<sup>p</sup>, W. Meyer<sup>q,2</sup>,  
 Z.-E. Meziani<sup>s</sup>, D. Miller<sup>k</sup>, G. Mitchell<sup>v</sup>, M. Olson<sup>g</sup>,  
 G. A. Peterson<sup>h</sup>, G. G. Petratos<sup>g</sup>, R. Pitthan<sup>q</sup>, R. Prepost<sup>v</sup>,  
 P. Raines<sup>m</sup>, B. A. Raue<sup>l,3</sup>, D. Reyna<sup>a</sup>, L. S. Rochester<sup>q</sup>,  
 S. E. Rock<sup>a</sup>, M. V. Romalis<sup>n</sup>, F. Sabatie<sup>f</sup>, G. Shapiro<sup>c</sup>,  
 J. Shaw<sup>h</sup>, T. B. Smith<sup>i</sup>, L. Sorrell<sup>a</sup>, P. A. Souder<sup>r</sup>, F. Staley<sup>f</sup>,  
 S. St. Lorant<sup>q</sup>, L. M. Stuart<sup>q</sup>, F. Suekane<sup>t</sup>, Z. M. Szalata<sup>a</sup>,  
 Y. Terrien<sup>f</sup>, A. K. Thompson<sup>j</sup>, T. Toole<sup>a</sup>, X. Wang<sup>r</sup>,  
 J. W. Watson<sup>g</sup>, R. C. Welsh<sup>i</sup>, F. R. Wesselmann<sup>l</sup>, T. Wright<sup>v</sup>,  
 C. C. Young<sup>q</sup>, B. Youngman<sup>q</sup>, H. Yuta<sup>t</sup>, W.-M. Zhang<sup>g</sup> and  
 P. Zyla<sup>s</sup>

<sup>a</sup>*The American University, Washington D.C. 20016*

<sup>b</sup>*Université Blaise Pascal, LPC IN2P3/CNRS, F-63170 Aubièrre Cedex, France*

<sup>c</sup>*University of California, Berkeley, California 94720-7300*

<sup>d</sup>*University of California, Los Angeles, California 90024*

<sup>e</sup>*California Institute of Technology, Pasadena, California 91125*

<sup>f</sup>*Centre d'Etudes de Saclay, DAPNIA/SPhN, F-91191 Gif-sur-Yvette, France*

<sup>g</sup>*Kent State University, Kent, Ohio 44242*

<sup>h</sup>*University of Massachusetts, Amherst, Massachusetts 01003*

<sup>i</sup>*University of Michigan, Ann Arbor, Michigan 48109*

<sup>j</sup>*National Institute of Standards and Technology, Gaithersburg, Maryland 20899*

<sup>k</sup>*Northwestern University, Evanston, Illinois 60201*

<sup>l</sup>*Old Dominion University, Norfolk, Virginia 23529*

<sup>m</sup>*University of Pennsylvania, Philadelphia, Pennsylvania 19104*

<sup>n</sup>*Princeton University, Princeton, New Jersey 08544*

<sup>o</sup>*Smith College, Northampton, Massachusetts 01063*

<sup>p</sup>*Southern Oregon State College, Ashland, Oregon 97520*

<sup>q</sup>*Stanford Linear Accelerator Center, Stanford, California 94309*

<sup>r</sup>*Syracuse University, Syracuse, New York 13210*

<sup>s</sup>*Temple University, Philadelphia, Pennsylvania 19122*

<sup>t</sup>*Tohoku University, Aramaki Aza Aoba, Sendai, Miyagi, Japan*

<sup>u</sup>*College of William and Mary, Williamsburg, Virginia 23187*

<sup>v</sup>*University of Wisconsin, Madison, Wisconsin 53706*

We present a Next-to-Leading order perturbative QCD analysis of world data on the spin dependent structure functions  $g_1^p$ ,  $g_1^n$ , and  $g_1^d$ , including the new experimental information on the  $Q^2$  dependence of  $g_1^n$ . Careful attention is paid to the experimental and theoretical uncertainties. The data constrain the first moments of the polarized valence quark distributions, but only qualitatively constrain the polarized sea quark and gluon distributions. The NLO results are used to determine the  $Q^2$  dependence of the ratio  $g_1/F_1$  and evolve the experimental data to a constant  $Q^2 = 5 \text{ GeV}^2$ . We determine the first moments of the polarized structure functions of the proton and neutron and find agreement with the Bjorken sum rule.

---

<sup>1</sup> Permanent Address: Institut des Sciences Nucléaires, IN2P3/CNRS, 38026 Grenoble Cedex, France

<sup>2</sup> Permanent Address: University of Bochum, D-44780 Bochum, Germany

<sup>3</sup> Present Address: Florida International University, Miami, FL 33199

## 1 Introduction

Next-to-Leading Order (NLO) perturbative QCD (pQCD) analyses of unpolarized lepton-nucleon deep inelastic scattering (DIS) [1–3] have resulted in the decomposition of the structure functions into valence quarks, sea quarks (of each flavor), and gluons. The data upon which these analyses are based include the scattering of charged leptons, neutrinos, and antineutrinos off a variety of targets, including both protons and deuterons, over a large kinematic range in both Bjorken  $x$  and momentum transfer  $Q^2$ .

Presently data are also available for polarized DIS [4–14]. Values for the polarized structure functions  $g_1(x)$  have been measured for protons, neutrons, and deuterons over a reasonable region of  $x$  and  $Q^2$  with good precision. Analyses of the first moments of the structure functions,  $\Gamma_1 = \int g_1(x)dx$ , have indicated that relatively little of the spin of the nucleon is carried by the quarks, suggesting that perhaps the sea quarks and gluons are polarized. Hence it is desirable to decompose the spin-dependent structure functions into contributions from valence quarks, antiquarks, and gluons just as has been done for the spin-averaged structure functions.

On the theoretical side, a full calculation of the Next-to-Leading Order (NLO) spin-dependent anomalous dimensions has been recently completed [15]. This provides for a perturbative QCD analysis of polarized DIS as a tool for decomposing the structure functions [16–19]. However, the lack of polarized neutrino data and the limited kinematic coverage in  $x$  and  $Q^2$  of the polarized DIS data limits the conclusions that can be drawn.

We have recently reported on a precision measurement of the neutron spin-dependent structure function  $g_1^n$  at an average four-momentum transfer squared  $Q^2 = 5 \text{ GeV}^2$  in SLAC experiment E154 [13]. The two independent spectrometers used in E154 provided a possibility of studying the  $Q^2$  dependence of the structure function  $g_1^n$ , and extended the kinematic range of the measurement beyond that of the previous SLAC experiments [7–10] to  $0.014 \leq x \leq 0.7$  and  $1 \text{ GeV}^2 \leq Q^2 \leq 17 \text{ GeV}^2$ . The E154 results presented in this Letter supplement our previously published data [13]. They currently constitute the most precise determination of  $g_1^n$ .

Of special interest for our data is the observation that the absolute value of  $g_1^n$  increases rapidly as  $x$  becomes small for  $x < 0.1$ , approximately as  $x^{-0.9}$  [13]. This is in striking contrast with the assumption of Regge behavior, which suggests that  $g_1^n$  is constant or decreases in magnitude with decreasing  $x$  [20]. Moreover, if the observed  $x$ -dependence of  $g_1^n$  persists to  $x = 0$ , the first moment  $\Gamma_1^n$  becomes unrealistically large.

We will show that by using NLO pQCD and reasonable assumptions about the

relation of the polarized and unpolarized distributions, we can obtain excellent fits to our data which can be used to determine the first moments  $\Gamma_1^p$  and  $\Gamma_1^n$ . Based on these fits, we evaluate what we know about the polarization of gluons and sea quarks. Careful attention is paid to the theoretical and experimental errors involved in the analysis.

## 2 Formalism

In the QCD-improved quark-parton model (QPM), the polarized structure function  $g_1(x)$  of the nucleon is related to the polarized quark, antiquark, and gluon distributions  $\Delta q(x)$ ,  $\Delta \bar{q}(x)$ , and  $\Delta G(x)$  via the factorization theorem [21]

$$g_1(x, Q^2) = \frac{1}{2} \sum_q^{N_f} e_q^2 \left[ C_q \otimes (\Delta q + \Delta \bar{q}) + \frac{1}{N_f} C_G \otimes \Delta G \right] \quad (1)$$

with the convolution  $\otimes$  defined as

$$(C \otimes q)(x, Q^2) = \int_x^1 \frac{dz}{z} C\left(\frac{x}{z}, \alpha_S\right) q(z, Q^2). \quad (2)$$

The sum is over all active quark flavors  $N_f$ .

The first moments of the structure functions of the proton and neutron,  $\Gamma_1^p$  and  $\Gamma_1^n$ , allow one to test the fundamental Bjorken sum rule [22] and determine the helicity content of the proton. The information on the  $x$  and  $Q^2$  dependence gives insight into the perturbative and non-perturbative dynamics of quarks and gluons inside the nucleon. Coefficient functions  $C_{q,G}(x, \alpha_S)$  correspond to the hard scattering photon-quark and photon-gluon cross sections and are referred to as Wilson coefficients. They are calculated in pQCD as an expansion in powers of the strong coupling constant  $\alpha_S$ . In leading order,  $C_q^{(0)} = \delta(1-x)$  and  $C_G^{(0)} = 0$  according to the simple partonic picture. The polarized NLO coefficient functions  $C_q^{(1)}$  and  $C_G^{(1)}$  in the modified minimal subtraction ( $\overline{\text{MS}}$ ) renormalization and factorization schemes are given in Ref. [15]. Throughout this paper, we use the fixed-flavor scheme [2,16] and set  $N_f = 3$  in Eq. (1). The heavy quark contributions are included in the running of the strong coupling constant  $\alpha_S(Q^2)$  calculated to two loops [23]. For consistency with the evolution of the unpolarized distributions, we adopt the values of  $\alpha_S(Q^2)$  and current quark masses from Ref. [2] that correspond to  $\alpha_S(M_Z^2) = 0.109$  or  $\alpha_S(5 \text{ GeV}^2) = 0.237$ . We include the uncertainty associated with the value of  $\alpha_S$  as will be discussed below. The parton distributions

in Eq. (1) are those of the proton. The neutron structure function is obtained by the isospin interchange  $u \leftrightarrow d$ , and the deuteron structure function is defined as  $g_1^d = (1/2)(g_1^p + g_1^n)(1 - 1.5\omega_D)$ , where the  $D$ -state probability  $\omega_D = 0.05 \pm 0.01$  [24].

The  $Q^2$  evolution of the parton densities is governed by the DGLAP equations [25]

$$Q^2 \frac{d}{dQ^2} \Delta q_{\text{NS}}^\eta(x, Q^2) = \frac{\alpha_S(Q^2)}{2\pi} P_{\text{NS}}^\eta \otimes \Delta q_{\text{NS}}^\eta, \quad \eta = \pm 1$$

and  $Q^2 \frac{d}{dQ^2} \begin{pmatrix} \Delta \Sigma(x, Q^2) \\ \Delta G(x, Q^2) \end{pmatrix} = \frac{\alpha_S(Q^2)}{2\pi} \begin{pmatrix} P_{qq} & P_{qG} \\ P_{Gq} & P_{GG} \end{pmatrix} \otimes \begin{pmatrix} \Delta \Sigma \\ \Delta G \end{pmatrix}, \quad (3)$

where the index NS stands for the the non-singlet quark distributions: valence  $\Delta u_V(x, Q^2) = \Delta u - \Delta \bar{u}$ ,  $\Delta d_V(x, Q^2) = \Delta d - \Delta \bar{d}$ , and the  $\text{SU}(3)_{\text{flavor}}$  non-singlet combinations  $\Delta q_3(x, Q^2) = (\Delta u + \Delta \bar{u}) - (\Delta d + \Delta \bar{d})$  and  $\Delta q_8(x, Q^2) = (\Delta u + \Delta \bar{u}) + (\Delta d + \Delta \bar{d}) - 2(\Delta s + \Delta \bar{s})$ . The  $\text{SU}(3)_{\text{flavor}}$  singlet distribution is  $\Delta \Sigma(x, Q^2) = (\Delta u + \Delta \bar{u}) + (\Delta d + \Delta \bar{d}) + (\Delta s + \Delta \bar{s})$ . The index  $\eta = 1$  refers to the evolution of the valence (charge-conjugation odd) distributions  $u_V$  and  $d_V$ , and  $\eta = -1$  refers to the evolution of the charge-conjugation even combinations  $\Delta q_3$ ,  $\Delta q_8$ , and  $\Delta \Sigma$ . The splitting functions  $P_{\text{NS}}^\eta$  and  $P_{ij}$  are calculated perturbatively with the leading order functions given in Ref. [25], and the next-to-leading order expressions recently obtained in Ref. [15]. In leading order, the evolution of both types of non-singlet distributions is the same:  $P_{\text{NS}}^{(0)\eta=-1} = P_{\text{NS}}^{(0)\eta=+1} = P_{qq}^{(0)}$  and the differences only appear in next-to-leading order. Starting with a parametrization of the parton densities at low initial scale  $Q_0^2 = 0.34 \text{ GeV}^2$ , the distributions at any value of  $Q^2 > Q_0^2$  are obtained using the solutions of the NLO DGLAP equations in the Mellin  $n$ -moment space [26,27]. The structure functions evolved in Mellin space are inverted back to Bjorken  $x$  space using the prescription of Ref. [27].

One of the conventions relevant to the interpretation of the deep inelastic scattering data at next-to-leading order arises from the relative freedom in defining the hard scattering cross sections  $C_{q,G}^{(1)}$  and the singlet quark density  $\Delta \Sigma$  in Eq. (1), known as the factorization scheme dependence [26,28,29]. In the unpolarized case, the factorization scheme is fixed by specifying the renormalization procedure for the hard scattering cross sections  $C_{q,G}$  [26,29]. In the polarized case, the situation is further complicated by the freedom in the definition of the  $\gamma_5$  matrix and the Levi-Civita tensor in  $n \neq 4$  dimensions [28,30] in dimensional regularization [31]. The NLO splitting functions and Wilson coefficients are given in Ref. [15] in the  $\overline{\text{MS}}$  scheme with the definition of the  $\gamma_5$  matrix following Ref. [31]. The specific feature of this scheme is that the first moment of the gluon coefficient function vanishes  $C_G^{(1)}(n=1) = 0$ , and the gluon density does not contribute to the integral of  $g_1$ . Several authors [32–

34] have advocated using a different factorization scheme in which the axial anomaly contribution  $-(\alpha_S(Q^2)/4\pi) \sum_q e_q^2 \Delta G$  is included in the integral  $\Gamma_1$ . The suggestion generated a vivid theoretical debate [28,32–35]. Such a scheme was referred to in Ref. [17] as the Adler–Bardeen (AB) scheme. In the AB scheme the total quark helicity is redefined compared to the  $\overline{\text{MS}}$  scheme

$$\begin{aligned}\Delta\Sigma_{\text{AB}} &= \Delta q_0(Q^2) + \frac{N_f \alpha_S(Q^2)}{2\pi} \Delta G(Q^2) , \\ \Delta\Sigma_{\overline{\text{MS}}} &= \Delta q_0(Q^2) ,\end{aligned}\tag{4}$$

where  $\Delta q_0$  is the proton matrix element of the  $\text{SU}(3)_{\text{flavor}}$  singlet axial current. An attractive feature of the AB scheme is that  $\Delta\Sigma_{\text{AB}}$  is independent of  $Q^2$  even beyond the leading order. One could also resurrect the naive QPM expectation  $\Delta\Sigma \approx 0.6 - 0.7$  and explain the violation of the Ellis-Jaffe sum rule if the product  $\alpha_S(Q^2)\Delta G(Q^2)$  turned out to be large [32–34].

The product  $\alpha_S(Q^2)\Delta G(Q^2)$  is scale-independent in the leading order since its anomalous dimension expansion starts at order  $\alpha_S^2$  [36]. This implies that as  $\alpha_S$  decreases logarithmically with  $Q^2$ ,  $\Delta G$  grows as  $1/\alpha_S(Q^2)$ . This growth is compensated by the increasing (with opposite sign) orbital angular momentum contribution  $\langle L_z \rangle$  [37,38] in order to satisfy the sum rule

$$\frac{1}{2}\Delta\Sigma + \Delta G + \langle L_z \rangle = \frac{1}{2}.\tag{5}$$

The gauge-invariant and scheme-independent formulation of this sum rule has recently been presented in Ref. [39].

Another consequence is that the ambiguity in the definition of the total quark helicity in Eq. (4) does not vanish at infinite  $Q^2$ . However, as long as the factorization and renormalization schemes are used consistently, NLO predictions can be made for the spin dependent structure functions and other hadronic processes involving spin degrees of freedom once the parton distributions are determined in one scheme and at one scale.

A transformation from the  $\overline{\text{MS}}$  scheme of t’Hooft and Veltman [31] to the AB scheme was constructed in Ref. [17]. This scheme is a simple modification of  $\overline{\text{MS}}$  since it preserves the low and high  $x$  behavior of the coefficient functions and anomalous dimensions, and thus the asymptotic behavior of parton distributions is not modified. In order to demonstrate the effects of the factorization scheme dependence, we perform our calculations in both  $\overline{\text{MS}}$  and AB schemes.

### 3 Fits

Following Ref. [16], we make our central ansatz of parametrizing the polarized parton distribution at the low initial scale  $Q_0^2 = 0.34 \text{ GeV}^2$  as follows:

$$\Delta f(x, Q_0^2) = A_f x^{\alpha_f} (1-x)^{\beta_f} f(x, Q_0^2), \quad (6)$$

where  $\Delta f = \Delta u_V, \Delta d_V, \Delta \bar{Q}, \Delta G$  are the polarized valence, sea, and gluon distributions (see below for the definition of  $\Delta \bar{Q}$ ), and  $f(x, Q_0^2)$  are the unpolarized parton distributions from Ref. [2]. The parametrization assumes the power-like asymptotic behavior of the polarized distributions at low  $x$  and low  $Q^2$ , namely  $\Delta f \sim x^{\gamma_f}$ ,  $x \rightarrow 0$ , where  $\gamma_f$  is the sum of the polarized power  $\alpha_f$  and the low  $x$  power of the unpolarized distribution. Since inclusive deep inelastic scattering does not provide sufficient information about the flavor separation of the polarized sea, we assume an ‘‘isospin-symmetric’’ sea  $\Delta \bar{u} = \Delta \bar{d} \equiv \frac{1}{2} (\Delta \bar{u} + \Delta \bar{d})$ . Under this assumption, the sea quark contribution to the polarized structure functions of the proton and neutron is the same:

$$g_1^{p \text{ sea}} = g_1^{n \text{ sea}} = (5/9)C_q \otimes [1/2(\Delta \bar{u} + \Delta \bar{d}) + 1/5\Delta \bar{s}]. \quad (7)$$

Inclusive DIS does not probe the light and strange sea independently. The only sensitivity to the difference between  $\Delta \bar{u}$ ,  $\Delta \bar{d}$ , and  $\Delta \bar{s}$  comes from the difference in the evolution of the two types of non-singlet distributions ( $\eta = \pm 1$  in Eq. (3)). Such a difference is beyond the reach of present-day experiments. Hence, we will parametrize a particular combination of the sea quark distributions that appears in Eq. (7):

$$\Delta \bar{Q} \equiv 1/2(\Delta \bar{u} + \Delta \bar{d}) + 1/5\Delta \bar{s}. \quad (8)$$

Furthermore, we assume the  $x$  dependence of the polarized strange and light sea to be the same, and fix the normalization of the strange sea by

$$\Delta s = \Delta \bar{s} = \lambda_s \frac{\Delta \bar{u} + \Delta \bar{d}}{2} = \frac{\lambda_s}{1 + \lambda_s/5} \Delta \bar{Q}, \quad (9)$$

with the  $SU(3)_{\text{flavor}}$  symmetry breaking parameter  $\lambda_s$  varying between 1 and 0 (where the latter choice corresponds to an unpolarized strange sea).

The positivity constraint,  $|\Delta f(x)| \leq f(x)$ , satisfied (within uncertainties) at the initial scale  $Q_0^2$ , holds at all scales  $Q^2 > Q_0^2$ ; it leads to the constraints  $\alpha_f \geq 0$  and  $\beta_f \geq 0$ . In addition, we assume the helicity retention properties of

the parton distributions [40] that require<sup>4</sup>  $\beta_f = 0$ . Unlike most NLO analyses [16–18], we do not assume  $SU(3)_{\text{flavor}}$  symmetry and do not fix the normalization of the non-singlet distributions by the axial charges  $\Delta q_3 = F + D$  and  $\Delta q_8 = 3F - D$ , where  $F$  and  $D$  are the antisymmetric and symmetric  $SU(3)$  coupling constants of hyperon beta decays [41]. Thus, we are able to test the Bjorken sum rule. In addition, the structure functions are not sensitive to the corrections beyond NLO in the data range.

The remaining eight coefficients are determined by fitting the available data on the spin dependent structure functions  $g_1^{p,n,d}$  of the proton [6,8,10,11], neutron [7,13,14], and deuteron [9,10,12] with  $Q^2 > 1 \text{ GeV}^2$ . We use either the results for  $g_1$  or determine the structure functions at the experimental values of  $Q^2$  using the results for  $g_1/F_1$  [42]. The unpolarized structure function  $F_1$  is obtained from a recent parametrization of  $F_2(x, Q^2)$  from NMC [43] and a fit to the data on  $R(x, Q^2)$ , the ratio of longitudinal to transverse photoabsorption cross sections from SLAC [44]. The weight of each point is determined by the statistical error. The best fit coefficients are listed in Table 1. The total  $\chi^2$  of the fits are 146 and 148 for 168 points in  $\overline{\text{MS}}$  and AB schemes, respectively.

The statistical errors on extracted parton densities  $\Delta q(x, Q^2)$ ,  $\Delta \bar{q}(x, Q^2)$ , and  $\Delta G(x, Q^2)$  were calculated by adding in quadrature statistical contributions from experimental points. The weight of each point was obtained by varying the point within its statistical error and calculating the change in the parton density [45]. The systematic error is usually dominated by the normalization errors (target and beam polarizations, dilution factors, etc.). Thus the systematic errors are to a large extent correlated point to point within one experiment<sup>5</sup>. We therefore assumed 100% correlated systematic errors for any given experiment and added systematic contributions within one experiment linearly. Systematic errors for each experiment were then added quadratically to obtain systematic uncertainties on parton densities.

The biggest source of theoretical uncertainty comes from the uncertainty on the value of  $\alpha_S$ . We estimate it by repeating the fits<sup>6</sup> with  $\alpha_S(M_Z^2)$  varied in the range allowed by the unpolarized fixed target DIS experiments [23]  $\alpha_S(M_Z^2) = 0.108 - 0.116$ . The quality of the fits deteriorated significantly when the values as high as  $\alpha_S(M_Z^2) = 0.120$  were used. The scale uncertainty is included in the error on  $\alpha_S$ . We also vary current quark masses in the range  $m_c = 1 - 2 \text{ GeV}$  and  $m_b = 4 - 5 \text{ GeV}$  which affects the running of  $\alpha_S$ . The effect of  $SU(3)_{\text{flavor}}$  breaking is estimated by varying the parameter  $\lambda_s$  from 1 to 0. These factors are found to have a small influence on the results. To test the sensitivity to the shape of the initial distributions and the value of the

<sup>4</sup> We have checked that the data are consistent with this assumption.

<sup>5</sup> This includes both proton and deuteron data taken in a single experiment, such as E143 and SMC.

<sup>6</sup> We also relax the positivity constraints.



starting scale  $Q_0^2$ , we repeat the fit with initial unpolarized distributions taken from Ref. [1] at  $Q_0^2 = 1 \text{ GeV}^2$  and find the results consistent with values given in Tables 1 and 2 within quoted statistical uncertainties. Possible higher twist effects are neglected since they are expected to drop with the photon-nucleon invariant mass squared  $W^2$  as  $1/W^2$  [46]. The cut  $W^2 > 4 \text{ GeV}^2$  has been applied to all the data with the majority of them exceeding  $W^2 > 8 \text{ GeV}^2$ .

## 4 Results and discussion

Results for the structure functions of the proton and neutron  $g_1^p$  and  $g_1^n$  at  $5 \text{ GeV}^2$  are compared to the experimental data in Fig. 1. Despite a small number of free parameters, the fits are excellent. In addition, at the initial scale  $Q^2 = 0.34 \text{ GeV}^2$  the low  $x$  behavior of the distributions is consistent with the Regge theory prediction  $\gamma_f \approx 0$  [20]. However, Regge theory in the past has been applied at the  $Q^2 \sim 2 - 10 \text{ GeV}^2$  of the experiments. This procedure clearly cannot be applied to the E154 neutron data for  $0.014 < x < 0.1$ , and is incompatible with the pQCD predictions [47,48]. If instead, Regge theory is assumed to apply at our starting  $Q^2$  to fix the values of powers  $\gamma_f$  to anywhere between 0 and 1, the data are fit with four parameters. Two of those parameters control the small contributions of gluons and antiquarks. When these parameters are fixed to zero, the resulting fit *with only two free parameters* still provides a reasonable description of the data everywhere except the low  $x$  region where it underestimates the E154 data on  $g_1^n$  by about two standard deviations.

The values of the first moments of parton distributions, as well as the first moments of structure functions at  $Q^2 = 5 \text{ GeV}^2$ , are given in Table 2. The procedure of fitting structure functions to power laws at low  $Q^2 = 0.34 \text{ GeV}^2$  evolved up to the experimental  $Q^2$  results in low  $x$  behavior that can be integrated to yield the first moments. If instead, the data are fit to a power law in  $x$  at the average  $Q^2 \approx 5 \text{ GeV}^2$ , a significantly bigger first moment of  $g_1^n$  is obtained [45]. Hence our results for the first moments depend strongly on the assumptions that we make regarding the low  $x$  behavior. However, the simple assumptions that we made are attractive theoretically and have remarkable predictive power.

The first moment of the deuteron structure function  $g_1^d$  that we obtain is smaller than that of Ref. [9]. The reason is that our assumptions about the low  $x$  behavior of  $g_1$  result in a contribution beyond the measured region of  $\int_0^{0.03} g_1^d dx \approx -0.014$  as opposed to  $\approx +0.001$  estimated in Ref. [9] assuming Regge behavior at  $Q^2 = 3 \text{ GeV}^2$ . The first moment of  $g_1^p$  is numerically less sensitive to how the data are extrapolated.

The first moments of the valence quark distributions are determined well, but the moments of the sea quark and gluon distributions are only qualitatively constrained. We note that the contribution of the experimental systematic errors to the errors on the first moments of the parton distributions is comparable to the statistical contribution. The full error on the first moment of the gluon distribution  $\Delta G$  is bigger than quoted in Ref. [17] despite the fact that the new data from E154 were added. The theoretical uncertainty is also quite large; it could potentially be reduced if the simultaneous analysis of the unpolarized and polarized data was performed (including  $\alpha_S$  as one of the parameters). It is interesting to note that at  $Q^2 = 0.34 \text{ GeV}^2$  the orbital angular momentum contribution  $\langle L_z \rangle = -0.2_{-0.3}^{+0.7}$  is consistent with zero, *i.e.* helicities of quarks and gluons account for most of the nucleon spin. The results of the fits in both  $\overline{\text{MS}}$  and AB schemes are consistent within errors. The fits are significantly less stable in the AB scheme. Note that the values of the singlet axial charge  $\Delta q_0$  are essentially the same for fits in both schemes.

The contributions from the valence quarks  $g_1^{n \text{ valence}} = (1/18)C_q \otimes (\Delta u_V + 4\Delta d_V)$  and sea quarks and gluons  $g_1^{n \text{ sea+gluon}} = (5/9)C_q \otimes \Delta \bar{Q} + (1/9)C_G \otimes \Delta G$  to the neutron spin structure function at  $Q^2 = 5 \text{ GeV}^2$  are shown in Fig. 2. One can see that the sea and gluon contributions are larger than the valence contributions at  $x \approx 10^{-3}$ . Although the sea contributions to  $g_1^n$  are relatively modest in the E154 data range  $x > 0.01$ , the strong  $x$  dependence  $g_1^n \sim x^{-0.8}$  observed by E154 below  $x = 0.1$  is largely due the sea and gluon contributions. An observation of a negative value of  $g_1^n$  at lower  $x$  and higher  $Q^2$  would provide direct evidence of a polarized sea.

One may note an apparent  $\approx 2\sigma$  disagreement of  $\Delta q_3$  with the value extracted from the neutron beta-decay [23]  $\Delta q_3 = g_A = 1.2601 \pm 0.0025$ . This is due to the fact that the calculation is done in NLO, and the higher order corrections to the Bjorken sum rule are not taken into account. The corrections can be as large as 5% [49] at  $Q^2 \approx 5 \text{ GeV}^2$ . They would bring  $\Delta q_3$  in better agreement with the beta decay data. For consistency with the NLO approximation, we do not include this correction; it has no effect on the physical observable  $g_1$ .

Using the parametrization of the parton distributions, one can obtain the polarized structure function (Eq. (1)) and evolve the experimental data points to a common  $\langle Q^2 \rangle$  using the formula:

$$g_1^{\text{exp}}(x_i, \langle Q^2 \rangle) = g_1^{\text{exp}}(x_i, Q_i^2) - \Delta g_1^{\text{fit}}(x_i, Q_i^2, \langle Q^2 \rangle) \quad (10)$$

with

$$\Delta g_1^{\text{fit}}(x_i, Q_i^2, \langle Q^2 \rangle) = g_1^{\text{fit}}(x_i, Q_i^2) - g_1^{\text{fit}}(x_i, \langle Q^2 \rangle), \quad (11)$$

where  $g_1^{\text{exp}}(x_i, Q_i^2)$  is the structure function measured at the experimental kine-

matics, and  $g_1^{\text{fit}}$  is the fitted value. The errors on  $g_1^{\text{exp}}(x_i, \langle Q^2 \rangle)$  have three sources:

$$\sigma^2(g_1^{\text{exp}}(x_i, \langle Q^2 \rangle)) = \sigma^2(g_1^{\text{exp}})_{\text{stat.}} + \sigma^2(g_1^{\text{exp}})_{\text{syst.}} + \sigma^2(g_1)_{\text{evol.}} , \quad (12)$$

where statistical and systematic uncertainties take into account the correlation between  $g_1^{\text{exp}}(x_i, Q_i^2)$  and  $g_1^{\text{fit}}$ , and the evolution uncertainty includes only uncorrelated experimental uncertainties as well as theoretical uncertainties added in quadrature.

The data on the structure function  $g_1^n$  from two independent spectrometers used in E154 are given in Table 3. These results provide new information on the  $Q^2$  dependence of  $g_1^n$  and thus supplement our previously published data [13]. Table 3 also lists the E154 data points evolved to  $\langle Q^2 \rangle = 5 \text{ GeV}^2$  using the  $\overline{\text{MS}}$  parametrization. The NLO evolution is compared to the traditional assumption of scaling of  $g_1^n/F_1^n$  in Fig. 3. The difference is only slightly smaller than the precision of the present-day experiments. The effect on  $\Gamma_1^n$  is small only if the integral is evaluated at the average value of  $Q^2$  (as is usually done). The  $Q^2$  dependence of the ratio  $g_1/F_1$  is shown in Fig. 4. We plot the difference between the values of  $g_1/F_1$  at a given  $Q^2$  and  $Q^2 = 5 \text{ GeV}^2$  to which the SLAC data are evolved. For the neutron, the evolution of  $g_1^n$  is slower than that of  $F_1^n$ . Therefore, assuming scaling of  $g_1^n/F_1^n$ , one typically overestimates the absolute value of  $g_1^n(x, \langle Q^2 \rangle)$  at low  $x$  (where  $Q_i^2 < \langle Q^2 \rangle$ ), and underestimates it at high  $x$  (where  $Q_i^2 > \langle Q^2 \rangle$ ). The two effects approximately cancel for the integral over the measured range in the case of E154. However, the shape of the structure function at low  $x$  affects the extrapolation to  $x = 0$ . The effect of the perturbative evolution is qualitatively the same for the proton.

The data on  $g_1^n$  averaged between two spectrometers are given in Table 4. Integrating the data in the measured range, we obtain (at  $Q^2 = 5 \text{ GeV}^2$ )

$$\int_{0.014}^{0.7} dx g_1^n(x) = -0.035 \pm 0.003 \pm 0.005 \pm 0.001 , \quad (13)$$

where the first error is statistical, the second is systematic, and the third is due to the uncertainty in the evolution. This value agrees well with the number  $-0.036 \pm 0.004$  (stat.)  $\pm 0.005$  (syst.) [13] obtained assuming the  $Q^2$  independence of  $g_1^n/F_1^n$ . Using the  $\overline{\text{MS}}$  parametrization to evaluate the contributions from the unmeasured low and high  $x$  regions, we determine the first moment

$$\Gamma_1^n = -0.058 \pm 0.004 \text{ (stat.)} \pm 0.007 \text{ (syst.)} \pm 0.007 \text{ (evol.)} \quad (14)$$

at  $Q^2 = 5 \text{ GeV}^2$ .

The behavior of the purely non-singlet combination  $(g_1^p - g_1^n)(x)$  is expected to be softer at low  $x$  than its singlet counterpart [50]. Evolving the E154 neutron and E143 proton [8] data to  $Q^2 = 5 \text{ GeV}^2$  and using the  $\overline{\text{MS}}$  parametrization of Table 1 to determine the contributions from the unmeasured low and high  $x$  regions, we obtain for the Bjorken sum

$$\Gamma_1^{p-n}(5 \text{ GeV}^2) = \int_0^1 dx (g_1^p - g_1^n) = 0.171 \pm 0.005 \pm 0.010 \pm 0.006, \quad (15)$$

where the first error is statistical, the second is systematic, and the third is due to the uncertainty in the evolution and low  $x$  extrapolation. This value is in good agreement with the  $O(\alpha_S^3)$  [49] prediction 0.188 evaluated with  $\alpha_S(M_Z^2) = 0.109$ , and it also agrees very well with the value in Table 2 obtained by direct integration of the parton densities. The result is fairly insensitive to the details of the low- $x$  extrapolation which is well constrained by the data. The low  $x$  behavior in the non-singlet polarized sector is also relatively insensitive to the higher-order corrections [51]. On the other hand, the low- $x$  extrapolation of the proton and neutron integrals alone still relies on the assumption that the asymptotic behavior of sea quark and gluon distributions can be determined from the present data, and that the effects of higher-order resummations are small. These assumptions, and therefore the evaluation of the total quark helicity  $\Delta\Sigma$ , are on potentially weaker grounds. Precise higher energy data on the polarized structure functions of both proton and neutron are required to determine this quantity.

## 5 Conclusions and Outlook

Additional high precision data from SLAC experiment E155 on the polarized structure functions of the proton and deuteron will be important in understanding the spin structure of the nucleon. New results on the proton structure function  $g_1^p$  from SMC have recently been presented [52]. Also, the polarized electron-proton collider experiments proposed at HERA [53] would be of great importance in unraveling the low  $x$  behavior of the spin-dependent structure function  $g_1^p$ . Furthermore, polarized fixed-target experiments at the Next Linear Collider would determine the structure functions of both the proton and the neutron over a broad kinematic range [54], and thus compliment the HERA program. Extrapolations based on the fits in this paper suggest that  $g_1^n(x)$  will be large at low  $x$  and have a significant  $Q^2$  dependence. Observing  $g_1^p$  become negative at low  $x$  would provide direct evidence of a polarized sea.

In conclusion, we have performed a Next-to-Leading order QCD analysis of the world data on polarized deep inelastic scattering. The data constrain the

first moments of the polarized valence quark distributions; the polarized gluon and sea quark distributions can only be qualitatively constrained. We determine that the  $Q^2$  dependence of the ratio  $g_1/F_1$  for the proton and neutron is sizable compared to present experimental uncertainties. We use the NLO pQCD evolution to determine the first moments of the spin dependent structure functions of the proton and neutron at  $Q^2 = 5 \text{ GeV}^2$ , and find that the data agrees with the Bjorken sum rule within one standard deviation.

We thank the SLAC accelerator department the successful operation of the E154 Experiment. We would also like to thank A. V. Manohar for reviewing the manuscript and valuable comments and W. Vogelsang and S. Forte for stimulating discussions. This work was supported by the Department of Energy; by the National Science Foundation; by the Kent State University Research Council (GGP); by the Jeffress Memorial Trust (KAG); by the Centre National de la Recherche Scientifique and the Commissariat a l'Energie Atomique (French groups); and by the Japanese Ministry of Education, Science and Culture (Tohoku).

## References

- [1] A. D. Martin, R. G. Roberts, and W. J. Stirling, Phys. Lett. B387 (1996) 419.
- [2] M. Glück, E. Reya, and A. Vogt, Z. Phys. C67 (1995) 433.
- [3] J. Botts *et al.*, Phys. Lett. B304 (1993) 159.
- [4] The E80 Collaboration, M. J. Alguard *et al.*, Phys. Rev. Lett. 37 (1976) 1261, 41, (1978) 70.
- [5] The E130 Collaboration, G. Baum *et al.*, Phys. Rev. Lett. 51 (1983) 1135.
- [6] The EMC Collaboration, J. Ashman *et al.*, Phys. Lett. B206 (1988) 364, Nucl. Phys. B328 (1990) 1.
- [7] The E142 Collaboration, P. L. Anthony *et al.*, Phys. Rev. Lett. 71 (1993) 959; Phys. Rev. D54 (1996) 6620.
- [8] The E143 Collaboration, K. Abe *et al.*, Phys. Rev. Lett. 74 (1995) 346.
- [9] The E143 Collaboration, K. Abe *et al.*, Phys. Rev. Lett. 75 (1995) 25.
- [10] The E143 Collaboration, K. Abe *et al.*, Phys. Lett. B364 (1995) 61.
- [11] The SMC Collaboration, D. Adams *et al.*, Phys. Lett. B329 (1994) 399; preprint hep-ex/9702005 (1997), submitted to Phys. Rev. D.
- [12] The SMC Collaboration, B. Adeva *et al.*, Phys. Lett. B302 (1993) 533; D. Adams *et al.*, Phys. Lett. B357 (1995) 248; Phys. Lett. B396 (1997) 338.

- [13] The E154 Collaboration, K. Abe *et al.*, preprint SLAC-PUB-7459, to be published in Phys. Rev. Lett. (1997).
- [14] The HERMES Collaboration, K. Ackerstaff *et al.*, preprint hep-ex/9703005 (1997), submitted to Phys. Lett. B.
- [15] R. Mertig and W.L. van Neerven, Z. Phys. C70 (1996) 637;  
W. Vogelsang, Phys. Rev. D54 (1996) 2023.
- [16] M. Glück *et al.*, Phys. Rev. D53 (1996) 4775.
- [17] R. D. Ball, S. Forte, and G. Ridolfi, Phys. Lett. B378 (1996) 255.
- [18] T. Gehrmann and W. J. Stirling, Phys. Rev. D53 (1996) 6100.
- [19] G. Altarelli *et al.*, preprint CERN-TH/96-345, submitted to Nucl. Phys. B.
- [20] R. L. Heimann, Nucl. Phys. B64 (1973) 429.
- [21] H. Georgi and H. D. Politzer, Phys. Rev. D9 (1974) 416;  
D. J. Gross and F. Wilczek, Phys. Rev. D9 (1974) 980.
- [22] J. D. Bjorken, Phys. Rev. 148 (1966) 1467; Phys. Rev. D1 (1970) 1376.
- [23] Review of Particle Properties, Particle Data Group (R. M. Barnett *et al.*), Phys. Rev. D55 (1996) 1.
- [24] M. Lacombe *et al.*, Phys. Rev. C21 (1980) 861;  
M. J. Zuilhof and J. A. Tjon, Phys. Rev. C22 (1980) 2369;  
R. R. Machleid *et al.*, Phys. Rep. 149 (1987) 1.
- [25] V. N. Gribov and L. N. Lipatov, Sov. J. Nucl. Phys. 15 (1972) 438, **15** (1972) 675;  
Yu. L. Dokshitzer, Sov. Phys. JETP 46 (1977) 461;  
G. Altarelli and G. Parisi, Nucl. Phys. B126 (1977) 298.
- [26] W. Furmanski and R. Petronzio, Z. Phys. C11 (1982) 293.
- [27] M. Glück, E. Reya, and A. Vogt, Z. Phys. C48 (1990) 471.
- [28] G. T. Bodwin and J. Qiu, in: Proc. of Polarized Collider Workshop (University Park, PA, 1990);  
G. T. Bodwin and J. Qiu, Phys. Rev. D41 (1990) 2755.
- [29] J. Chyla, Phys. Rev. D48 (1993) 4385.
- [30] A. V. Manohar, Phys. Rev. Lett. 65 (1990) 2511.
- [31] G. t'Hooft and M. Veltman, Nucl. Phys. B44 (1972) 189.
- [32] A. V. Efremov and O. V. Teryaev, JINR-E2-88-287 (1988); Phys. Lett. B240 (1990) 200.
- [33] G. Altarelli and G. Ross, Phys. Lett. B212 (1988) 391.
- [34] R. D. Carlitz, J. D. Collins and A. H. Mueller, Phys. Lett. B214 (1988) 229.

- [35] R. L. Jaffe and A. V. Manohar, Nucl. Phys. B337 (1990) 509;  
A. V. Manohar, Phys. Rev. Lett. 66 (1991) 289.
- [36] J. Kodaira, Nucl. Phys. B165 (1980) 129.
- [37] M. Anselmino, A. Efremov, and E. Leader, Phys. Rep. 261 (1995) 1.
- [38] P. Ratcliffe, Phys. Lett. B192 (1987) 309.
- [39] X. Ji, J. Tang, and P. Hoodbhoy, Phys. Rev. Lett. 76 (1996) 740;  
X. Ji, Phys. Rev. Lett. 78 (1997) 610.
- [40] S. J. Brodsky, M. Burkardt, and I. Schmidt, Nucl. Phys. B441 (1994) 197.
- [41] M. Bourquin *et al.*, Z. Phys. C21 (1983) 27.
- [42] The formulae are summarized in: T. Pussieux and R. Windmolders, in: Internal Spin Structure of the Nucleon, ed. V. W. Hughes and C. Cavata (World Scientific, 1995)
- [43] M. Arneodo *et al.*, Phys. Lett. B364 (1995) 107.
- [44] L. W. Whitlow *et al.*, Phys. Lett. B250 (1990) 193; S. Dasu *et al.*, Phys. Rev. D49 (1994) 5641.
- [45] Yu. G. Kolomensky, Ph. D. Thesis, University of Massachusetts (1997), unpublished.
- [46] S. J. Brodsky *et al.*, Nucl. Phys. B369 (1992) 519.
- [47] M. A. Ahmed and G. G. Ross, Phys. Lett. B56 (1975) 385;  
M. B. Einhorn and J. Soffer, Nucl. Phys. B74 (1986) 714.
- [48] R. D. Ball, S. Forte, and G. Ridolfi, Nucl. Phys. B444 (1996) 287.
- [49] S. G. Gorishny and S. A. Larin, Phys. Lett. B172 (1986) 109;  
S. A. Larin and J. A. M. Vermaseren, Phys. Lett. B259 (1991) 345.
- [50] J. Bartels, B. I. Ermolaev, and M. G. Ryskin, Z. Phys. C70 (1996) 273.
- [51] J. Blümlein, S. Riemersma, and A. Vogt, preprint DESY-96-131 (1996);  
Nucl. Phys. Proc. Suppl. 51C (1996) 30.
- [52] B. Derro, in: Proc. 32nd Rencontres de Moriond: QCD and High-Energy Hadronic Interactions (Moriond, 1997), to be published in the proceedings.
- [53] R. D. Ball *et al.*; A. De Roeck *et al.*, in: Proc. Workshop on Future Physics at HERA, (Hamburg, 1995–1996), ed. G. Ingelman, A. De Roeck, and R. Klanner (DESY, 1996).
- [54] E. W. Hughes, in: Proc. 12th Int. Symposium on High Energy Spin Physics, SPIN '96 (Amsterdam, 1996), to be published in the proceedings.

Table 1

Fitted values of the free parameters in Eq. (6) in  $\overline{\text{MS}}$  and AB schemes. Also quoted are the statistical, systematic, and theoretical errors.

	$\overline{\text{MS}}$				AB			
	Value	Stat.	Syst.	Theory	Value	Stat.	Syst.	Theory
$A_u$	0.99	+0.08 -0.08	+0.04 -0.05	+0.97 -0.11	0.98	+0.07 -0.06	+0.05 -0.07	+0.96 -0.09
$A_d$	-0.78	+0.14 -0.20	+0.05 -0.05	+0.05 -1.28	-0.82	+0.06 -0.11	+0.07 -0.06	+0.31 -1.21
$A_Q$	-0.02	+0.03 -0.06	+0.01 -0.02	+0.01 -0.35	-0.04	+0.02 -0.05	+0.01 -0.02	+0.03 -0.06
$A_G$	1.6	+1.1 -0.9	+0.6 -0.6	+0.2 -1.3	0.1	+1.0 -0.3	+0.5 -0.2	+0.1 -0.6
$\alpha_u$	0.63	+0.06 -0.07	+0.04 -0.05	+0.36 -0.06	0.55	+0.08 -0.06	+0.03 -0.04	+0.56 -0.05
$\alpha_d$	0.28	+0.15 -0.11	+0.05 -0.03	+0.75 -0.03	0.40	+0.20 -0.12	+0.07 -0.13	+0.53 -0.34
$\alpha_Q$	0.04	+0.29 -0.03	+0.12 -0.03	+0.55 -0.01	0.00	+0.17 -0.00	+0.17 -0.00	+0.00 -0.00
$\alpha_G$	0.8	+0.4 -0.5	+0.3 -0.3	+0.1 -0.6	0.0	+0.7 -0.0	+1.0 -0.0	+1.0 -0.0

Table 2

First moments of the polarized parton distributions and structure functions of the proton, neutron, and deuteron in  $\overline{\text{MS}}$  and AB schemes evaluated at  $Q^2 = 5 \text{ GeV}^2$ . Errors are statistical, systematic, and theoretical.

	$\overline{\text{MS}}$				AB			
	Value	Stat.	Syst.	Theory	Value	Stat.	Syst.	Theory
$\Delta_{uV}$	0.69	+0.03 -0.02	+0.05 -0.04	+0.14 -0.01	0.74	+0.03 -0.02	+0.03 -0.03	+0.07 -0.01
$\Delta_{dV}$	-0.40	+0.03 -0.04	+0.03 -0.03	+0.07 -0.00	-0.33	+0.03 -0.04	+0.03 -0.05	+0.01 -0.03
$\Delta_{\bar{Q}}$	-0.02	+0.01 -0.02	+0.01 -0.01	+0.00 -0.03	-0.03	+0.02 -0.02	+0.01 -0.01	+0.01 -0.01
$\Delta_G$	1.8	+0.6 -0.7	+0.4 -0.5	+0.1 -0.6	0.4	+1.0 -0.7	+0.9 -0.6	+1.1 -0.1
$\Delta_{q_3}$	1.09	+0.03 -0.02	+0.05 -0.05	+0.06 -0.01	1.07	+0.03 -0.02	+0.06 -0.06	+0.10 -0.01
$\Delta_{q_8}$	0.30	+0.06 -0.05	+0.05 -0.05	+0.23 -0.01	0.42	+0.05 -0.08	+0.06 -0.06	+0.03 -0.01
$\Delta_\Sigma$	0.20	+0.05 -0.06	+0.04 -0.05	+0.01 -0.01	0.25	+0.07 -0.07	+0.05 -0.05	+0.05 -0.02
$\Delta_{q_0}$	0.20	+0.05 -0.06	+0.04 -0.05	+0.01 -0.01	0.21	+0.05 -0.06	+0.06 -0.07	+0.05 -0.02
$\Gamma_1^p$	0.112	+0.006 -0.006	+0.008 -0.008	+0.009 -0.001	0.114	+0.005 -0.006	+0.010 -0.011	+0.001 -0.003
$\Gamma_1^n$	-0.056	+0.006 -0.007	+0.005 -0.006	+0.002 -0.001	-0.051	+0.005 -0.006	+0.006 -0.007	+0.001 -0.012
$\Gamma_1^d$	0.026	+0.005 -0.006	+0.005 -0.006	+0.005 -0.001	0.029	+0.004 -0.005	+0.007 -0.008	+0.001 -0.007
$\Gamma_1^{p-n}$	0.168	+0.005 -0.004	+0.008 -0.007	+0.007 -0.001	0.165	+0.004 -0.004	+0.009 -0.009	+0.013 -0.001



Table 3

E154 results on  $g_1^n$  at the  $Q^2$  of the measurement for each spectrometer. Also shown are results for  $g_1^n$  evolved to  $\langle Q^2 \rangle = 5 \text{ GeV}^2$  according to Eq. (10). Errors were propagated as described in the text.

$x_i$	$Q_i^2$ GeV <sup>2</sup>	$g_1^n(x_i, Q_i^2)$ ± stat. ± syst.	$g_1^n(x_i, 5 \text{ GeV}^2)$ ± stat. ± syst. ± evol.
2.75° spectrometer			
0.017	1.2	-0.351 ± 0.115 ± 0.109	-0.421 ± 0.115 ± 0.113 ± 0.016
0.024	1.6	-0.374 ± 0.071 ± 0.064	-0.409 ± 0.071 ± 0.066 ± 0.007
0.035	2.0	-0.289 ± 0.061 ± 0.038	-0.304 ± 0.061 ± 0.039 ± 0.005
0.049	2.6	-0.212 ± 0.041 ± 0.022	-0.215 ± 0.041 ± 0.023 ± 0.004
0.078	3.3	-0.119 ± 0.031 ± 0.013	-0.117 ± 0.031 ± 0.013 ± 0.002
0.123	4.1	-0.075 ± 0.030 ± 0.010	-0.073 ± 0.030 ± 0.010 ± 0.001
0.173	4.6	-0.070 ± 0.033 ± 0.010	-0.069 ± 0.033 ± 0.010 ± 0.001
0.241	5.1	-0.053 ± 0.028 ± 0.008	-0.053 ± 0.028 ± 0.008 ± 0.000
0.340	5.5	0.002 ± 0.036 ± 0.004	0.001 ± 0.036 ± 0.004 ± 0.000
0.423	5.8	0.027 ± 0.059 ± 0.007	0.027 ± 0.059 ± 0.007 ± 0.000
5.5° Spectrometer			
0.084	5.5	-0.152 ± 0.029 ± 0.019	-0.153 ± 0.029 ± 0.019 ± 0.001
0.123	7.2	-0.117 ± 0.017 ± 0.013	-0.121 ± 0.017 ± 0.013 ± 0.002
0.172	8.9	-0.059 ± 0.016 ± 0.009	-0.066 ± 0.016 ± 0.009 ± 0.003
0.242	10.7	-0.040 ± 0.012 ± 0.006	-0.047 ± 0.012 ± 0.006 ± 0.003
0.342	12.6	-0.019 ± 0.012 ± 0.005	-0.024 ± 0.012 ± 0.005 ± 0.001
0.442	13.8	-0.009 ± 0.012 ± 0.003	-0.011 ± 0.012 ± 0.003 ± 0.001
0.564	15.0	0.003 ± 0.008 ± 0.001	0.003 ± 0.008 ± 0.001 ± 0.000

Table 4

Combined results on  $g_1^n$  at the  $Q^2$  of the measurement. Also shown are results for  $g_1^n$  evolved to  $\langle Q^2 \rangle = 5 \text{ GeV}^2$  according to Eq. (10).

$x_i$	$Q_i^2$	$g_1^n(x_i, Q_i^2)$		$g_1^n(x_i, 5 \text{ GeV}^2)$		
	GeV <sup>2</sup>	± stat.	± syst.	± stat.	± syst.	± evol.
0.017	1.2	-0.351 ± 0.115	± 0.109	-0.421 ± 0.115	± 0.113	± 0.016
0.024	1.6	-0.374 ± 0.071	± 0.064	-0.409 ± 0.071	± 0.066	± 0.007
0.035	2.0	-0.289 ± 0.061	± 0.038	-0.304 ± 0.061	± 0.039	± 0.005
0.049	2.6	-0.204 ± 0.040	± 0.022	-0.207 ± 0.040	± 0.023	± 0.004
0.081	4.5	-0.137 ± 0.021	± 0.016	-0.136 ± 0.021	± 0.016	± 0.002
0.123	6.6	-0.108 ± 0.015	± 0.012	-0.111 ± 0.015	± 0.012	± 0.002
0.173	8.2	-0.061 ± 0.014	± 0.009	-0.067 ± 0.014	± 0.009	± 0.003
0.242	9.8	-0.042 ± 0.011	± 0.007	-0.048 ± 0.011	± 0.007	± 0.003
0.342	11.7	-0.017 ± 0.011	± 0.005	-0.021 ± 0.011	± 0.005	± 0.001
0.441	13.3	-0.007 ± 0.011	± 0.002	-0.009 ± 0.011	± 0.002	± 0.001
0.564	15.0	0.003 ± 0.008	± 0.001	0.003 ± 0.008	± 0.001	± 0.000

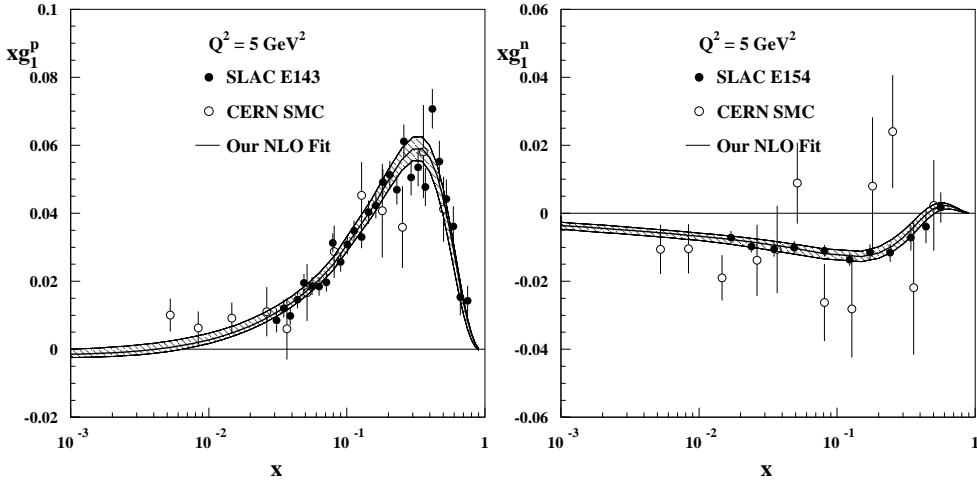


Fig. 1. The structure functions  $xg_1^p$  and  $xg_1^n$  at  $Q^2 = 5 \text{ GeV}^2$ . The E143, SMC, and E154 data have been evolved to  $Q^2 = 5 \text{ GeV}^2$  using a procedure described in the text. The result of the  $\overline{\text{MS}}$  fit is shown by the solid line and the hatched area represents the total error of the fit.

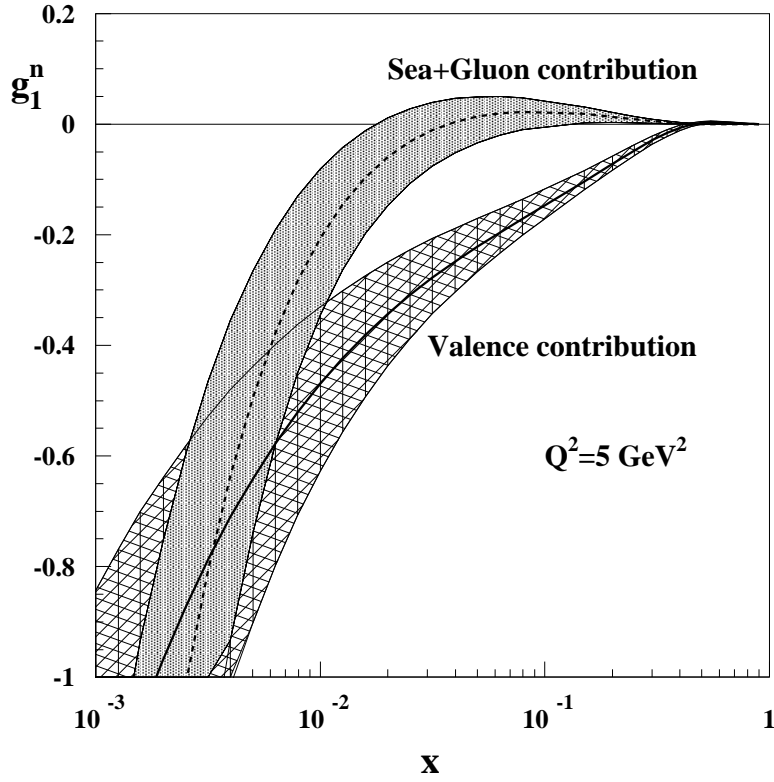


Fig. 2. The contributions to the structure function  $g_1^n$  of the neutron from the valence quarks  $[(1/18)C_q \otimes (\Delta u_V + 4\Delta d_V)]$  (solid line) and from the sea quarks and gluons  $[(5/9)C_q \otimes \Delta \bar{Q} + (1/9)C_G \otimes \Delta G]$  (dashed line). The shaded and hatched areas represent the total uncertainties on each quantity.

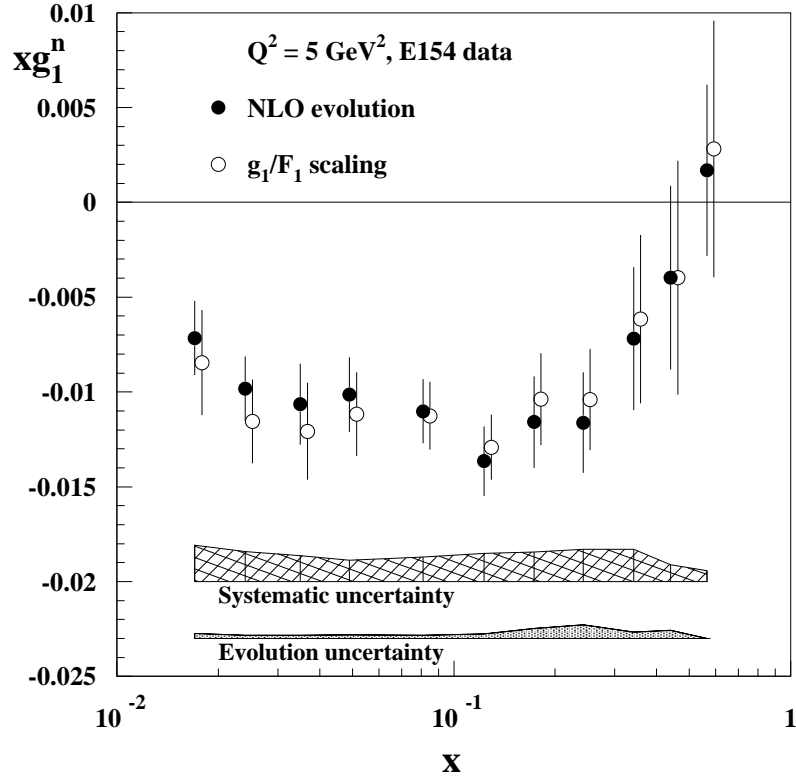


Fig. 3. The structure function  $xg_1^n$  evolved to  $Q^2 = 5 \text{ GeV}^2$  using our  $\overline{\text{MS}}$  parametrization and using the assumption that  $g_1^n/F_1^n$  is independent of  $Q^2$ .

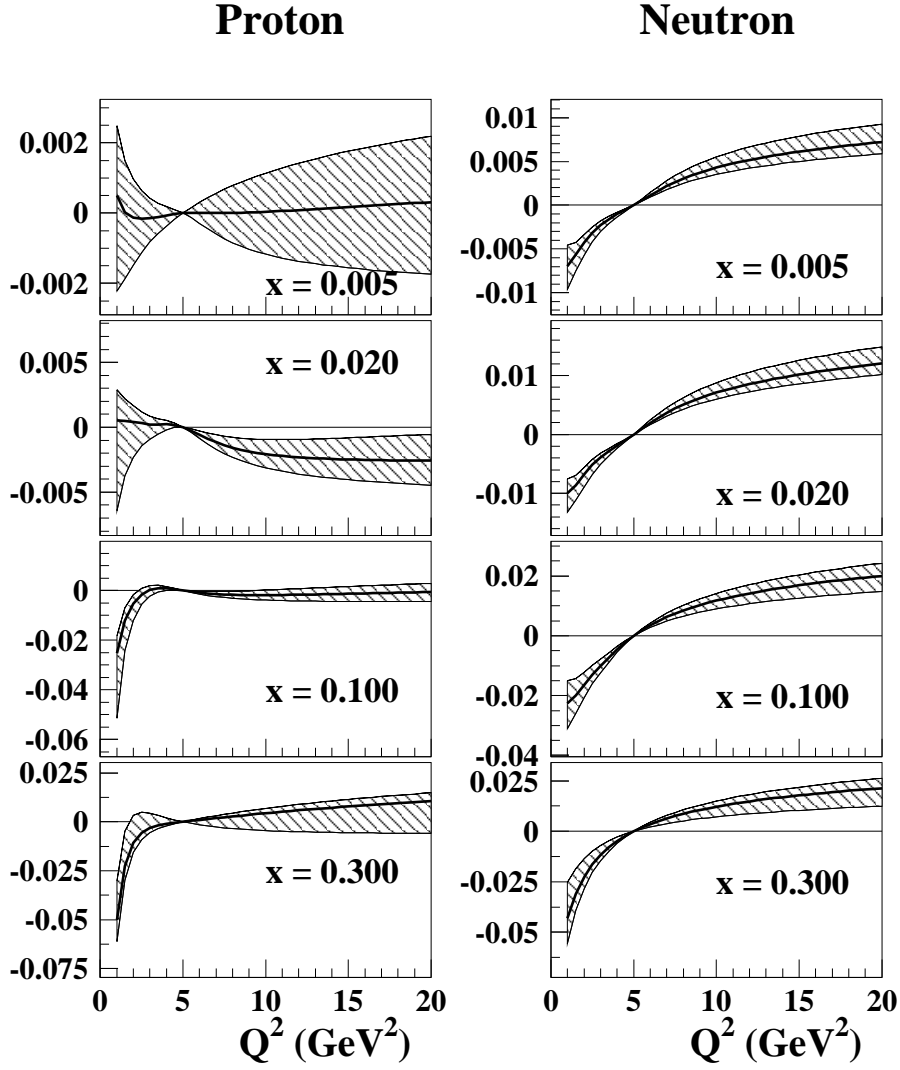


Fig. 4. Evolution of the ratios  $g_1/F_1$  for proton (left) and neutron (right). Plotted is the difference  $\frac{g_1}{F_1}(x, Q^2) - \frac{g_1}{F_1}(x, 5 \text{ GeV}^2)$ . The  $\overline{\text{MS}}$  fit is shown by the solid line and the hatched area represents the total (experimental and theoretical) uncertainty of the fit.